applied sciences

MDPI

Article

Spider Silk-Augmented Scaffolds and Adipose-Derived Stromal Cells Loaded with Uniaxial Cyclic Strain: First Investigations of a Novel Approach for Tendon-Like Constructs

Frederik Schlottmann [1,*], Sarah Strauss [1], Christian Plaass [2], Bastian Welke [3], Peter M. Vogt [1] and Joern W. Kuhbier [1,†]

[1] Department of Plastic, Aesthetic, Hand- and Reconstructive Surgery, Hannover Medical School, Carl-Neuberg-Strasse 1, 30625 Hannover, Germany; strauss.sarah@mh-hannover.de (S.S.); vogt.peter@mh-hannover.de (P.M.V.); JoernWolfram.Kuhbier@diakovere.de (J.W.K.)

[2] Diakovere Annastift, Orthopedic Clinic of the Hannover Medical School, Anna-von-Borries-Strasse 1-7, 30625 Hannover, Germany; christian.plaass@diakovere.de

[3] Laboratory for Biomechanics and Biomaterials, Department of Orthopedics, Hannover Medical School, Anna-von-Borries-Strasse 1-7, 30625 Hannover, Germany; welke.bastian@mh-hannover.de

* Correspondence: schlottmann.frederik@mh-hannover.de; Tel.: +49-511-532-0

† Current address: Joern W Kuhbier, Department of Plastic, Hand and Micro Surgery, Diakovere Friederikenstift, Humboldtstrasse 5, 30169 Hannover, Germany.

Abstract: Tendon injuries still pose a challenge to reconstructive surgeons. Tendon tissue is a bradytrophic tissue and has a poor tendency to heal. Autologous tendon grafts are, therefore, still the gold standard in restorative operations but are associated with significant donor side morbidity. The experimental approach of the present study focused on the use of the biomaterial spider silk as a biocompatible and very stable carrier matrix in combination with a collagen type I hydrogel and adipose-derived stromal cells. The constructs were differentiated by axial strain to tendon-like tissue using a custom-made bioreactor. Macroscopically, tendon-like tissue could be detected which histologically showed high cell vitality even in long-term cultivation. In addition, cell morphology comparable to tenocytes could be detected in the bioreactor-stimulated tendon-like constructs compared to the controls. Immunohistochemically, tendon tissue-specific markers could be detected. Therefore, the developed tendon-like construct represents a promising approach towards patient specific tendon reconstruction, but further studies are needed.

Keywords: tendon tissue engineering; spider silk scaffold; ASC; bioreactor; mechanotransduction

Citation: Schlottmann, F.; Strauss, S.; Plaass, C.; Welke, B.; Vogt, P.M.; Kuhbier, J.W. Spider Silk-Augmented Scaffolds and Adipose-Derived Stromal Cells Loaded with Uniaxial Cyclic Strain: First Investigations of a Novel Approach for Tendon-Like Constructs. *Appl. Sci.* **2021**, *11*, 1218. https://doi.org/10.3390/app11031218

Received: 19 December 2020
Accepted: 22 January 2021
Published: 28 January 2021

1. Introduction

Tendons and ligaments are among the most important structures in the locomotive system. They play a significant role in biomechanical stability and force transmission between muscle to bone (tendon) and bone to bone (ligament). While bone and cartilage tissues are hard tissue and have high compressive strength, ligaments and tendons are considered as soft tissue and have high tensile strength [1]. While bone and muscle have a high regenerative capacity, tendons and cartilage display slow and poor healing abilities, i.e., fibrotic scar healing in tendons and minimal to no healing at all in cartilage [2,3]. Tendons are specialized tissues with a relative hypocellularity, low vascularity, low metabolic rate and a resulting degree of hypoxia, which are required to bear tension for extended durations, but not to suffer ischemia and therefore necrosis [4]. Tendons have a poor natural healing capacity due to low cellularity and low vascularity and, therefore, prolonged and incomplete healing can cause a higher risk of re-injury or joint malfunction. Tendon injuries, representing a prevalent clinical picture, are responsible for considerable morbidity in athletes, working and elder populations and, therefore, causing significant social and economic costs for treatment, rehabilitation and prevention [5,6]. However, tendon

injuries are still a challenge for reconstructive surgery and, therefore, either restorative operations or versatile grafts are needed to fully replace their function. High failure and recurrence rates have implicated the usage of autograft, allograft and xenograft in tissue replacement [7]. Therefore tissue engineering of tendon tissue might play a significant role for future therapeutic strategies and clinical applications. Choosing the most favorable biomaterial as scaffold for tendon tissue engineering is still challenging as it has to have several features that could translate it into functional tendon tissue [8]. For tendon tissue engineering, mechanical stimulation by means of strain seemed to induce further differentiation in terms of cell shape, production of extracellular matrix (ECM) and expression of tissue-specific markers [9–12]. Applied strain results in straightening, realignment and sliding of tendon and, therefore, collagen fibers, ultimately subjecting tenocyte nuclei under strain [13,14]. This consecutively leads to interference of their mechanotransduction pathways and fibril alignment [15]. Studies focusing on bioreactor-based systems led to insights in engineering tendon-like constructs (TLC). Loading amplitudes affect cell and tissue properties with physiological loads leading to overall anabolic response and increased strength of the construct. In contrast, no mechanical stimulation or high amplitude loads lead to a catabolic response [16]. Probably the most favorable approaches are those based on functional tissue engineering with special regard to in vitro-to-in vivo strategies, which ultimately aim to allow early implantation while at the same time tolerate substantial in vivo forces early postoperatively and even larger forces once patients resume to normal activities of daily living [16]. Many biomaterials have been investigated as scaffold for tendon tissue engineering purposes including collagen, silk, alginate, chitosan, polycaprolactone, polyglycolic acid and polylactic acid. In addition, several techniques have been investigated, such as electrospinning, electrochemical alignment, knitting and freeze-drying to create tendon-like constructs [17]. However, current tendon tissue engineering approaches showed promising short-term results but failed over time. The ideal scaffold material should be biodegradable and biocompatible as well as providing sufficient mechanical properties [7,18]. The stability of the biomaterial chosen depends on mechanical strength, elasticity and biodegradation. Therefore, matching the mechanical properties of a scaffold to those of native ECM is important to ensure that tissue growth is not limited by mechanical failure of the scaffold [7]. Based on these necessities, a potential biomaterial for tissue engineering of tendon tissue could be spider silk due to its unrivaled biomechanical properties. As there are actually seven different types of silk with unique biomechanical features in each, the silk type with the properties most suitable to the desired tissue can be chosen [19]. For example, silk from the tubuliform gland, used for the outer egg cases, shows a porous structure and a high toughness in terms of energy to break (up to 1×10^9 J kg^{-1}), while dragline silk from the major ampullate gland has a unique tensile strength (up to 4×10^9 N m^{-1}) [20]. Additionally, spider silk has shown a very good biocompatibility in vitro and in vivo [21,22].

Adipose-derived stromal cells (ASC) represent a promising cell population for tissue engineering due to their easy accessibility [23]. Regarding tendon tissue engineering, successful approaches included ASC as well [24]. The concept of this study was to investigate spider drag line silk in combination with a collagen type I hydrogel as scaffolds for ASC in a bioreactor model using cyclic strain with the intention to engineer tendon-like tissue. Cell morphology and matrix composition were examined using histological staining. To prove differentiation of ASC into tenocytes, immunohistochemical staining for tendon specific markers was performed. Biomechanical testing indicated loading capacity of our tendon like construct. Overall, the present study can be considered as a pilot study.

2. Materials and Methods

2.1. Isolation and Expansion of Adipose-Derived Stromal Cells (ASC)

Human adipose-derived stromal cells were isolated from adipose tissue after abdominoplasty surgery from a female donor, aged 41 years, with informant consent of the patient and approval by the Ethics Committee of Hannover Medical School (Ethics Ap-

proval No. 3475-2017; Date of approval: 15 February 2017). Isolation and characterization of ASC were performed according to standardized methods described earlier [25]. Briefly, fat tissue was digested, centrifuged and seeded, followed by a washing off of the non-adherent cells. All experiments were performed to internal standardized protocols and followed good-manufacturing practice. Cells were cultured in Dulbecco's modified Eagle's growth medium (DMEM-F12) (Gibco, Life Technologies, Darmstadt, Germany) with L-glutamine and without phenol red, adding 10% (*v*/*v*) fetal bovine serum (FCS) (Biochrom, Berlin, Germany), 1% (*v*/*v*) 10,000 µg/mL penicillin and streptomycin (Biochrom, Berlin, Germany) and 0.1% (*v*/*v*) 50 mg/mL ascorbic acid-2-phosphate. ASC were incubated at 37 °C and 5% CO_2 in a humidified atmosphere. ASC of passage 1 were used for all experiments.

2.2. Isolation of Collagen Type I

Collagen type I was isolated from rat-tail tendons of 14-week-old male Lewis rats (Charles River, Wilmington, Massachusetts, USA) provided as donor animals for tail amputation and tendon preparation according to the German Animal Welfare Law. The rat-tails came as a contribution from the animal experiments of another work group. Collagen type I was isolated by acetic acid extraction. Briefly, a series of acidic dissolution and dialysis were performed, sterility tests confirmed sterile conditions [26]. Protein molecule size was characterized with 7.5% sodium dodecyl sulfate polyacrylamide gel (SDS-PAGE) electrophoresis. The SDS-PAGE gel was stained with GelCode® Blue Stain Reagent (Life Technologies, Darmstadt, Germany) according to the manufacturer instructions. The concentration of collagen was measured with a NanoDrop ND-1000 spectrophotometer (ThermoFisher Scientific, Walldorf, Germany) according to manufacturer instruction and as published elsewhere [27]. The soluble collagen type I with a final concentration of 6.22 mg/mL was stored at 4 °C prior to preparation of TLCs.

2.3. Animal Handling and Harvesting Procedure of Spider Silk

Studies including spiders as an invertebrate species do not require any ethical or legal approval according to the German Animal Welfare Law. Spiders of the species *Nephila edulis* were kept in 25 °C warm and humidified rooms in our local laboratory facilities [28]. Dragline silk from the major ampullate gland was harvested as described earlier [28,29]. The dragline silk was reeled 100 times around a custom-made stainless steel frame measuring 15.0 × 1.0 × 0.1 cm (Figure 1). The frames holding the silk were steam sterilized at 121 °C, 100% water saturation and 2 bar of pressure for 15 min prior to their further use.

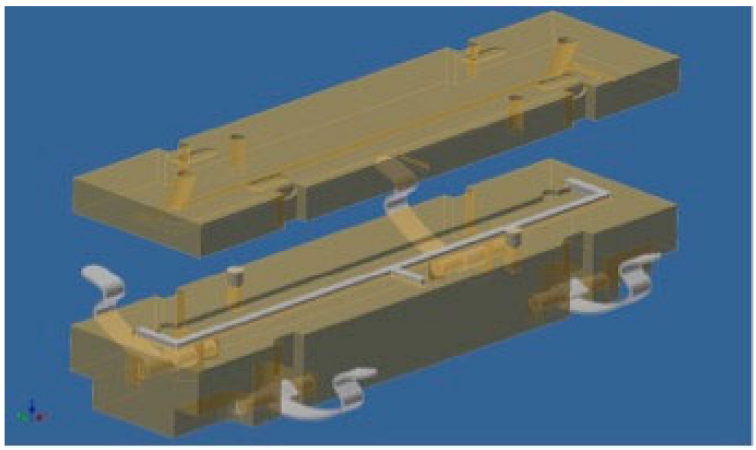

Figure 1. Custom-made casting chamber for fabrication of tendon-like constructs.

2.4. Preparation of Tendon-Like Constructs

To form a stable construct, a custom-made casting chamber made from teflon and steel was designed and manufactured in local facilities of the Central Research Devices Service

Unit of Hannover Medical School. The steel frames with the spider silk on them were clamped in the casting chambers and seeded under sterile conditions with 10 mL hydrogel composed of collagen type I and ASC dissolved in a solution of phosphate-buffered saline (PBS) (Gibco, Life Technologies, Darmstadt, Germany) and 10× concentrated DMEM-F12 (Biochrom, Berlin, Germany). 7.5% *v/v* sodium hydrogen carbonate solution (Sigma-Aldrich, St. Louis, MA, USA) was added to neutralize the collagen solution and achieve a final pH value of 7. Constructs were incubated for 90 min at 37 °C and 7% CO_2 (Figure 1). Steel frames with constructs were transferred to cell culture flasks afterwards and further incubated with DMEM-F12 medium. After 2 days of incubation, steel frames were cut off following another 7 days of incubation before either transferring the constructs to the custom-made bioreactor to undergo mechanical stressing or incubation for another 21 days. Cell culture medium was changed three times weekly. After in total 30 days of incubation, all constructs were processed for further examinations. Constructs where divided in 4 experimental groups as seen in Table 1.

Table 1. Overview of experimental groups for mechanical stimulation using the bioreactor and corresponding controls.

	Bioreactor (9 Days of Incubation Followed by 21 days of Mechanical Stimulation)	**Controls (9 Days of Incubation Followed by 21 days of Unstressed Culture)**
Constructs with spider silk	A (n = 6)	C (n = 6)
Constructs without spider silk	B (n = 6)	D (n = 6)

2.5. Contraction Assay

Prior to the first stressing using the bioreactor, contraction properties of collagen gels and the optimal number of cells required for experiments were determined by measuring contraction in width and length over a period of 30 days in constructs containing different numbers of ASC. Constructs were divided into 4 groups: 5.0×10^5 cells and spider silk, 5.0×10^5 cells without spider silk, 5.0×10^6 cells with spider silk and 5.0×10^6 without spider silk (Table 2). Every group consisted of 3 constructs to achieve comparable results. Constructs were incubated over a period of 30 days in DMEM-F12 medium, changing the medium three times weekly. No mechanical stress by use of the bioreactor was applied to observe contraction properties alone. Width and length were measured using a vernier caliper at days 0, 2, 9, 16, 23 and 30. All results were analyzed using Microsoft Excel software. The contraction properties are represented in the form of mean ± standard deviations. All further experiments were performed with 5.0×10^5 ASC.

Table 2. Overview of experimental groups for contraction assay with different numbers of adipose derived stromal cells (ASC)

	5.0×10^5 ASC	**5.0×10^6 ASC**
Constructs with spider silk	E (n = 3)	G (n = 3)
Constructs without spider silk	F (n = 3)	H (n = 3)

2.6. Concept of Bioreactor Cultivation and Mechanical Induction of Differentiation

Based on the conceptual design published earlier [30] an optimized and modified custom-made bioreactor system was designed (Figure 2) and built using Teflon, glass and stainless steel in local facilities of the Central Research Devices Service Unit of Hannover Medical School. The main component of the bioreactor was an incubation chamber made of glass, which could be hermetically sealed by means of a glass lid. A filter inserted in the lid allowed gas exchange. One mounting was fixed whereas the other was connected via the transmission shaft with the drive motor. In order to enable cyclic axial stressing of the constructs, they were suspended horizontally between two anchorages by means of two vessel clamps per construct on the metal pins provided for this purpose. The vessel clamps (Schwartz Micro Serrefine (Fine Science Tools, Heidelberg, Germany)) were used to

prevent the constructs from cutting into the metal pins during direct impaling. An external motor, which is not visible in Figure 2, controlled the drive shaft. Constructs underwent cyclic uniaxial stressing over a distance of 3 mm/sec (i.e., 2% strain from original length) for eight hours daily with a frequency of 1 Hz. A rest of 16 h followed every stressing. As described above, constructs were incubated nine days prior to mechanical stressing for 21 days to allow cell adhesion and proliferation. The medium was changed after two days under sterile conditions. Unstressed constructs were incubated in DMEM-F12 medium for 21 days instead and served as controls. After 30 days in total, constructs were processed for further histological examinations.

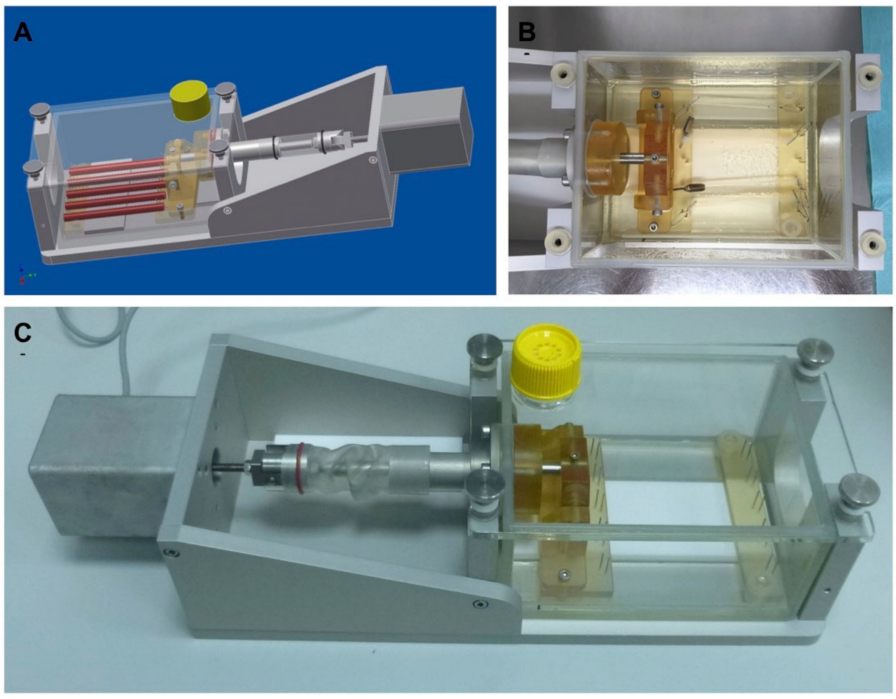

Figure 2. Custom-made bioreactor for uniaxial cyclic strain of tendon like constructs. (**A**): Design drawing of the bioreactor. (**B**): Top view of the bioreactor filled with constructs and cell medium. (**C**): General view of the bioreactor with drive motor, but without control unit.

2.7. Cell Viability Analysis

Cell viability in small pieces of tendon-like constructs of all experimental groups was evaluated using a LIVE/DEAD® Viability/Cytotoxicity Kit for mammalian cells (Life Technologies, Darmstadt, Germany) according to the manufacturer instructions. To reduce non-specific background staining, tissue pieces were washed with PBS prior to fluorescent microscopy with a Keyence BZ-8000K microscope (Keyence, Neu-Isenburg, Germany).

2.8. Histology

From every experimental group according to Table 1, samples measuring approximately 1.0 cm were collected for histological staining. Constructs were fixed with 4% buffered formalin (Carl Roth, Karlsruhe, Germany), dehydrated in a graded series of increasing alcohol concentrations, cleared in xylene, embedded in standard procedure in paraffin, and cut into 10 µm sections with a microtome (Microm International GmbH, Walldorf, Germany). Slides were deparaffinated, rehydrated by descendent alcohol concentrations and stained with Masson–Goldner Trichrome stain. The sections were first stained for 2 min in an iron hematoxylin solution consisting of iron hematoxylin A according to Weigert (Carl Roth GmbH, Karlsruhe, Germany) and iron hematoxylin B according to Weigert (Carl Roth GmbH, Karlsruhe, Germany) mixed in a 1:1 ratio immediately prior to staining. This was followed by blueing under running tap water for 15 min and rinsing in 0.5% (*v*/*v*) phosphotungstic acid for a few seconds. After washing in 1% (*v*/*v*) acetic

acid (Carl Roth GmbH, Karlsruhe, Germany) the cytoplasm was stained for 1 min with a Ponceau acid foxsin solution. The sections were washed again in double-distilled water and 1% (v/v) acetic acid before being stained for 10 min with a phosphotungstic acid orange G solution. In a final staining step, the collagenous connective tissue was stained with light green for 5 min after renewed washing with double-distilled water and 1% (v/v) acetic acid.

To exclude osteogenic mineralization and adipogenic differentiation of ASC, slides were stained with Oil Red O as specific adipogenic dye and Alizerin Red as specific osteogenic dye. Bright-field microscopy with a Keyence BZ-8000K microscope (Keyence, Neu-Isenburg, Germany) was performed to view stained sections. Oil Red O and Alizerin Red stains are not shown in the manuscript as no osteogenic or adipogenic differentiation could be observed.

2.9. Immunofluorescence Staining

To analyze protein expression levels within tendon-like tissue, indirect immunofluorescence staining was performed on paraffin embedded sections. A single sample was used for each immunofluorescence staining. Samples were permeated with 0.1% Tritron X-100 (Carl Roth, Karlsruhe, Germany) and blocked with 2% BSA. The primary antibodies used in this study were goat anti-human collagen I polyclonal antibody (abcam, Cambridge, UK), mouse anti-human collagen III monoclonal antibody (abcam, Cambridge, UK), rabbit anti-human Scleraxis polyclonal antibody (abcam, Cambridge, UK) as well as mouse anti-human Tenascin C monoclonal antibody (abcam, Cambridge, UK). Primary antibodies were applied for 1 h followed by extensive washing with PBS. Alexa Fluor® 488 conjugated chicken anti-rabbit antibody (ThermoFisher Scientific, Walldorf, Germany) and Alexa Fluor® 546 conjugated goat anti-mouse antibody (ThermoFisher Scientific, Walldorf, Germany) were used as secondary antibodies. Sections were covered and counterstained with 4′,6-diamidino-2-phenylindole (DAPI) according to the manufacturer's instructions. Inverse fluorescence microscopy with a Zeiss Axiovert 200 M microscope (Carl Zeiss, Oberkochen, Germany) was performed to view stained sections.

3. Results

In this study, a TLC was developed based on collagen type I hydrogel, ASC and spider silk scaffolds. Handmade spider silk scaffolds were seeded as mentioned with a combination of rat collagen type I hydrogel and ASC. Constructs were divided into 4 groups as seen in Table 1. All constructs were incubated 9 days prior to further incubation in either the bioreactor or cell culture to allow cell adhesion and proliferation. After 9 days, constructs of experimental groups A and B underwent mechanical stimulation using the bioreactor for 21 days to induce differentiation of ASC. Experimental groups C and D were unstressed and cultured for 21 days and therefore served as controls. Every experimental group consisted of 2 constructs per cycle and 3 cycles were performed, receiving 6 constructs per experimental group. After a total of 30 days of incubation, all constructs were processed for further examinations. Histological and immunohistochemical staining as well as live-dead assays were performed after 30 days.

3.1. Successful Preparation of Tendon-Like Constructs with 4×10^5 ASC and Collagen Type I Hydrogel

Drag line silk of spiders of the species *Nephila edulis* was harvested and collected on custom-made stainless steel frames. As described above, a custom-made casting chamber was used to form stable TLCs (Figure 1). Steel frames with or without spider silk were placed in the casting chamber and the lid was closed. The hydrogel composing of collagen I and ASC was added using a pipette. After 90 min of incubation, stable constructs were achieved that underwent further incubation prior to mechanical stimulation using the bioreactor.

Prior to first stressing using the bioreactor, contraction properties of collagen gels with and without spider silk as well as the optimal number of cells required for experiments were determined by measuring contraction characteristics of constructs. Table 2 displays an overview of experimental groups with different numbers of ASC for the contraction assay.

Every experimental group consisted of 3 constructs to achieve comparable results. A minimum length of 4.5 cm was required to ensure a stable fixation of constructs in the bioreactor for further experiments. After two days of incubation, steel frames were cut off following another 28 days of incubation. The medium was changed every two days. The measurement results of the contraction assay with respect to the length of TLC are displayed in Table 3. The results are shown as mean value with the corresponding standard deviation in cm. Figure 3 shows a graphical overview of the contraction assay with respect to the length shortening according to Table 2.

Table 3. Results of the contraction assay with respect to the length of tendon-like constructs (TLC). The results are shown as mean value with the corresponding standard deviation in cm.

Experimental Group (n = 3)	Day 0	Day 1	Day 2	Day 9	Day 16	Day 23	Day 30
E	15.00 ± 0.00	14.83 ± 0.29	13.70 ± 0.46	11.07 ± 0.23	7.23 ± 1.63	6.20 ± 2.18	5.73 ± 1.99
F	15.00 ± 0.00	14.83 ± 0.29	14.33 ± 0.21	11.10 ± 1.13	5.47 ± 1.24	5.00 ± 1.57	4.67 ± 1.78
G	15.00 ± 0.00	15.00 ± 0.00	13.00 ± 0.40	3.27 ± 0.32	2.63 ± 0.45	2.30 ± 0.17	2.07 ± 0.20
H	15.00 ± 0.00	15.00 ± 0.00	14.23 ± 0.30	5.20 ± 2.95	3.00 ± 0.36	2.50 ± 0.10	2.27 ± 0.15

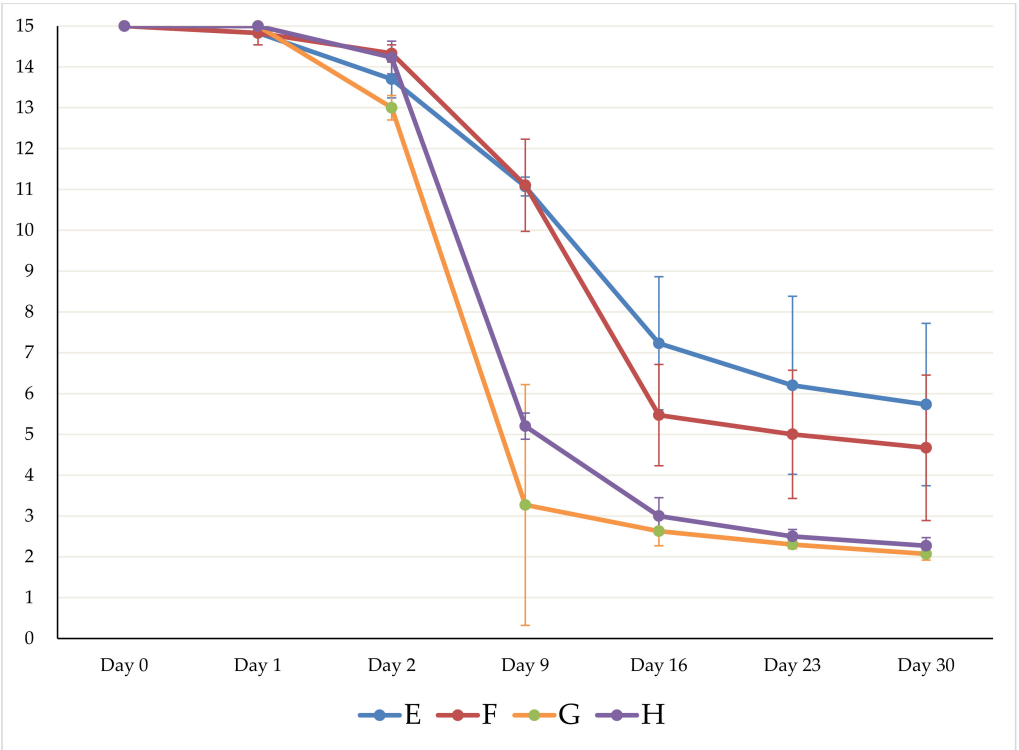

Figure 3. Graphical evaluation of the contraction assay with respect to the length shortening according to Table 2. Experimental group E: TLC with spider silk and 5.0×10^5 ASC. Experimental group F: TLC without spider silk and with 5.0×10^5 ASC. Experimental group G: TLC with spider silk and 5.0×10^6 ASC. Experimental group H: Construct without spider silk and with 5.0×10^6 ASC. All measurements were made as triplicate (n = 3) and are graphically shown as mean ± standard deviation.

As shown in Table 2 and Figure 3, the constructs with spider silk showed a more pronounced contraction with respect to length. In the averaged triplicate, constructs of experimental group E had shrunk to 38.2 ± 13.3% of their initial length whereas constructs

of experimental group F had shrunk to 31.1 ± 11.9% of their initial length after 30 days of incubation. In comparison, constructs of experimental group G had shrunk to 13.8 ± 1.3% of their initial length whereas constructs of experimental group H had shrunk to 15.1 ± 1.0% of their initial length. To sum up, constructs with 5×10^6 ASC showed a more pronounced contraction over the study period of 30 days. Constructs of experimental group G and H were too short to ensure a stable fixation of constructs in the bioreactor. Consequently, 5×10^5 ASC were used for all further experiments.

3.2. Mechanical Induction of ASC Differentiation Using the Custom-Made Bioreactor Showed Macroscopic Results Comparable to Tendon Tissue

As described above, custom-modified bioreactors were made and constructs stressed with a uniaxial strain. A total of five constructs could be cultivated in parallel in the bioreactor. Two constructs with spider silk (experimental group A) and two constructs without spider silk (experimental group B) were stressed in the bioreactor per cycle and the three cycles were performed in total. No bacterial contamination was observed over the experimental period of 30 days. It was macroscopically observed that constructs containing spider silk were more stable in handling. Furthermore, after 21 days of mechanical stressing the constructs showed a phenotype which had the first morphological signs that could be indicative of ASC differentiation towards tenocytes. No differences could be observed between experimental groups A and B (Figure 4).

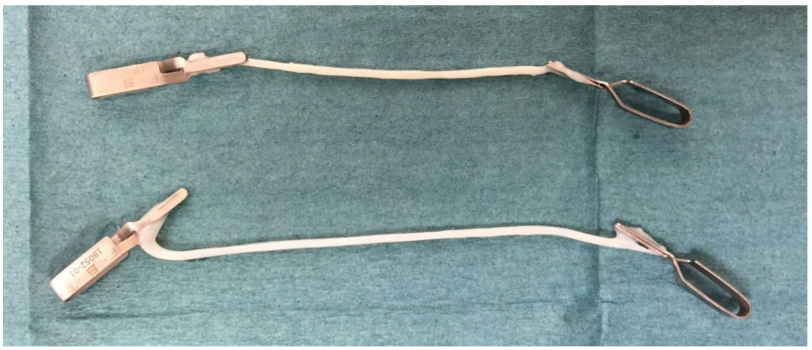

Figure 4. Tendon like constructs after 21 days of mechanical stressing using the bioreactor. The top one contains spider silk (experimental group A), the bottom one is manufactured without spider silk (experimental group B). The constructs showed phenotypes comparable to tendon tissue with no difference between experimental groups A and B.

3.3. Histological Analysis Shows Long-Term Cell Survival and Histological Patterns Comparable to Tendon Tissue

The LIVE/DEAD stain showed that the majority of cells were viable in all experimental and control groups after a period of 30 days (Figure 5). Only a negligible number of cells were dead. In addition, a low cell density was observed in all constructs and no significant differences between experimental groups could be detected. As seen in Figure 5A,C, truncated spider silk fibers showed a reddish autofluorescence. However, an orientation of cells and silk fibers towards the direction of mechanical stimulation was observed in experimental groups (Figure 5A,B). Compared to those constructs, controls showed a less aligned orientation of cells (Figure 5C,D). On trend, lower cell density was found in constructs with mechanical stimulation compared to those without mechanical stimulation.

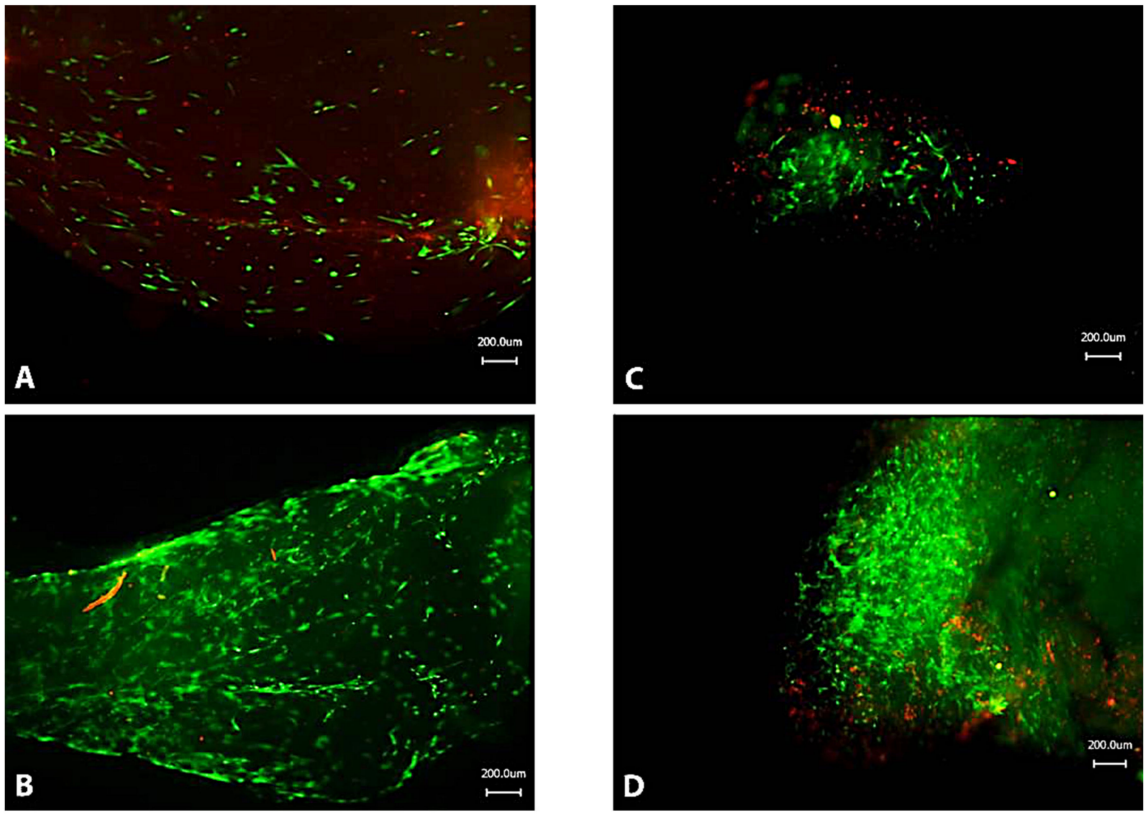

Figure 5. LIVE/DEAD-Assay of all experimental groups. Green fluorescent dye shows vital cells, red fluorescent dye indicates dead cells. (**A**)**.** Construct containing spider silk and bioreactor cultivation (experimental group A). (**B**). Construct without spider silk and with bioreactor cultivation (experimental group B). (**C**). Construct with spider silk and without mechanical stimulation (experimental group C). (**D**). Construct without spider silk and without mechanical stimulation (experimental group D).

In Masson–Golder Trichrome staining, microscopically collagenous connective tissue is green, the nuclei brown-black, the cytoplasm red and the muscles pale red. Elastic fibers often do not show a specific color and can be greenish or light red. The tendon-like constructs of the experimental group A showed a clear orientation of the collagen fibrils and the spider silk fibers along the direction of mechanical tension (Figure 6A). The cells showed an elongated cell phenotype comparable to tenocytes (Figure 6A). In experimental group B, collagen fibrils and spider silk fibers showed an orientation along the direction of the mechanical tension as well (Figure 6B). Overall, cells in the mechanically stimulated TLC showed a broad distribution within the matrix (Figure 6A,B) whereas the unstimulated controls showed the formation of coherent cell formations (Figure 6C,D).

Compared to experimental group A, cells showed an elongated cell phenotype as well but also formed coherent cell formations especially at the edges of the tendon-like constructs (Figure 6B). In experimental group C and D, collagen fibrils as well as spider silk fibers showed no coherent orientation and cells showed a more roundish phenotype (Figure 6C,D). As already seen in the LIVE/DEAD-Assay, a lower cell density was observed in stressed tendon-like constructs (Figure 6A,B) compared to unstressed controls (Figure 6C,D).

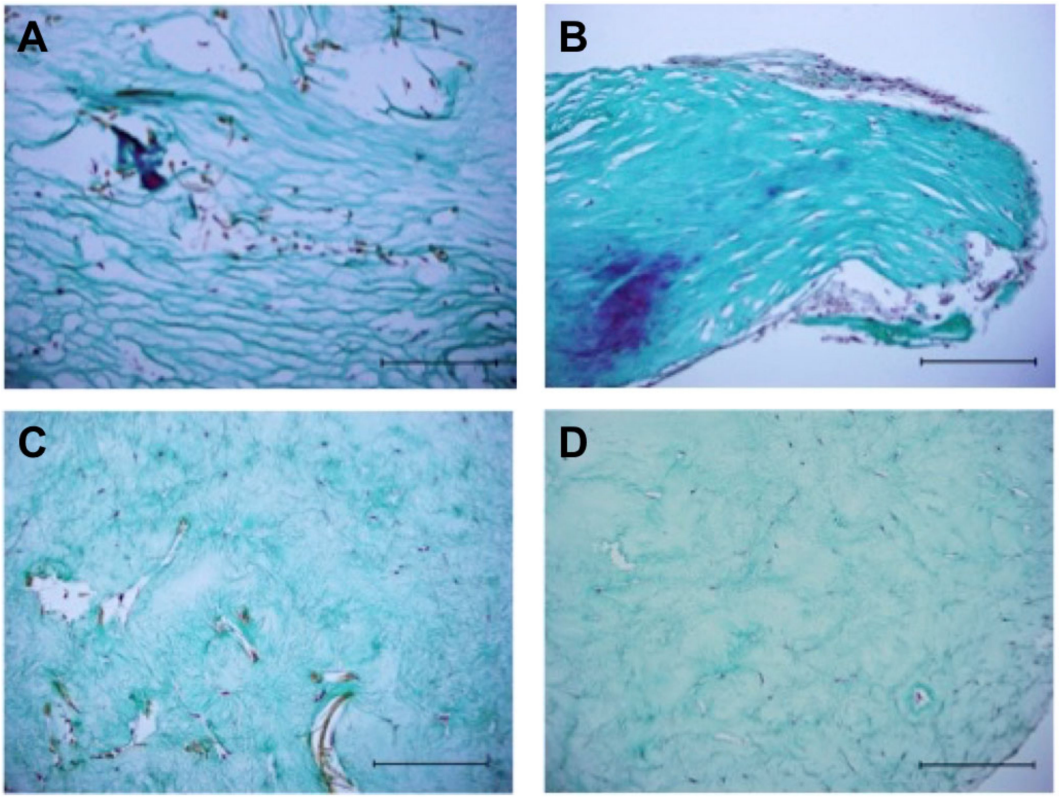

Figure 6. Masson–Goldner Trichrome stainings of all experimental groups. Collagenous connective tissue is stained green, the nuclei brown-black and the cytoplasm red. Elastic fibers often do not show a specific color and can be greenish or light red in color. The measuring bars represent 200 micrometers. (**A**). Construct containing spider silk and bioreactor cultivation (experimental group A). (**B**). Construct without spider silk and with bioreactor cultivation (experimental group B). (**C**). Construct with spider silk and without mechanical stimulation (experimental group C). (**D**). Construct without spider silk and without mechanical stimulation (experimental group D).

3.4. Immunohistochemical Staining Showed Production of Own Extracellular Matrix and Expression of Tendon Specific Markers

To analyze protein expression levels within TLC, indirect immunofluorescence staining was performed on paraffin embedded sections. Immunohistochemical staining was performed for human collagen I and III as well as Tenascin C and Scleraxis as tendon tissue-specific markers. Staining procedures followed standardized internal protocols and good manufacturing practice. The results are shown in Figure 7. Interestingly, Scleraxis could not be stained in any sample. As shown in Figure 7A, TLC showed the expression of human collagen I and III as well as Tenascin C after 21 days of mechanical stimulation in the bioreactor. TLC of experimental group B showed the expression of human collagen I and III as well as Tenascin C as shown in Figure 7B. Therefore, production of human extracellular matrix as well as expression of tendon specific markers can be postulated after mechanical induction of differentiation of ASC. As seen in Figure 7A,C, truncated spider silk fibers showed a reddish autofluorescence. As shown in Figure 7C,D, the unstressed TLC showed a significantly reduced immunofluorescence or only a background staining without staining of the target proteins.

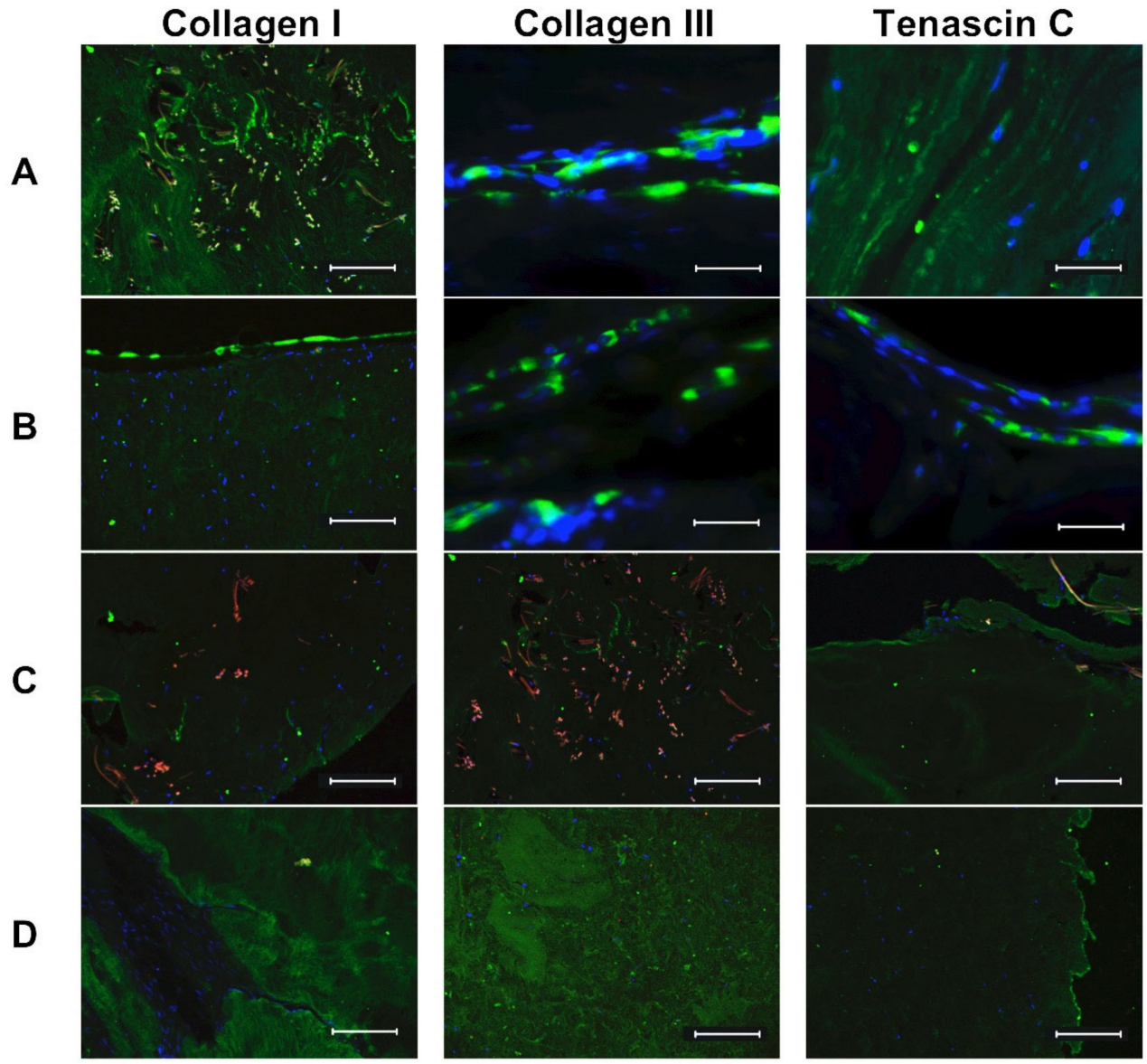

Figure 7. Results of the immunohistological staining. The cell nuclei were stained with 4′,6-diamidino-2-phenylindole (DAPI) and can be recognized by a blue fluorescence. The target proteins each show a green fluorescence. The spider silk shows a red autofluorescence. The measurement bars represent 200 micrometers. (**A**) Results of experimental group A. (**B**) Results of experimental group B. (**C**) Results of experimental group C. (**D**) Results of experimental group D.

4. Discussion

In the study at hand, we employed spider silk to stabilize collagen gels for tissue engineering of TLCs. To further improve cell distribution and induce mechanotransduction, cyclic uniaxial strain was applied. The frequency of the cyclic strain was with 1 Hz lower than the stride frequency found in equine canter, which is approximately 2 Hz, but comparable to the strain used by other studies, in particular for the promotion of stem cell differentiation towards tenocytes [31–33]. While some studies applied strain for as little as 15 to 20 min per 24 h, as 15 min per 24 h were sufficient for a notable effect regarding mechanical induction, longer application periods were suggested [33,34]. To mimic the mechanical requirements of daily life activities, we chose much longer periods (i.e., 8 h per day), however, an interesting concept for future research might be the investigation of changes due to different periods of strain application between 15 min and 8 h or several periods per day.

Biomechanical analysis of the TLCs in terms of traditional tensile testing was intended to be performed with a tensile test machine but turned out to be unsuccessful as TLCs displayed a fragile, soft and wet morphology and, therefore, were irrevocably damaged on loading in the tensile testing machine as it was described by other authors [33,35]. This is clearly a limitation of the feasibility study at hand which needs to be overcome by future studies further characterizing spider silk-based TLCs as a biomechanical similarity to the natural tissue is necessary. A possible solution might be involvement of dynamic shear analysis, dynamic scanning calorimetry or Fourier-transform infrared spectroscopy [26]. However, spectroscopic analysis might be susceptible to interference of autofluorescence of spider silk as described before [30]. Nevertheless, mechanical properties close to or surpassing the mechanical properties of natural tendon tissue can be assumed as spider silk (which functions as a stabilizing backbone for the constructs in this study) has been shown to possess extraordinary properties. For example, bundles of native spider silk were investigated as a tendon tissue suture and showed tensile strength comparable to polypropylene sutures and a superior resistance to mechanical fatigue [36].

Concerning the viability, most of the cells in the TLC were viable. Interestingly, further analysis revealed differences regarding cell morphology and distribution dependent on whether axial stimulation was present or not. In both TLCs with or without spider silk, cell distribution and morphology in constructs without mechanical stimulation were more likely to show a higher cell density with round cell bodies. In contrast, mechanical stimulation led to a lower cell density with tenocyte-like morphology. In mature tendons, two different zones can be distinguished: the gliding zone with chondrocyte-like cells at regions of pressure at the hypomochlion and the traction zone with elongated tenocytes parallel to the collagen fibers [37]. In the TLCs in this study, areas without mechanical stimulation displayed histological features of a gliding zone in tendons while those areas where uniaxial strain was applied displayed histological features of a traction zone. Therefore, the whole construct may be regarded as traction zone equivalent.

A red fluorescence was noticed in the LIVE/DEAD-Assay as well as in the immunofluorescence staining (Figures 5 and 7). This fluorescence might be caused either by autofluorescence of collagen type I or autofluorescence of spider silk. While spider silk displayed autofluorescence in the wavelength spectrum of 488 to 546 nm probably due to its amount of phosphorus [29,38], the autofluorescence spectrum of collagen caused by the amino acids tyrosine and tryptophan lies more in wavelength spectrum of 305–380 nm [39].

Cell contraction in collagen gels has been described before [40], but could be only divided into two phases contrary to the three phases of native cells. As in the study at hand, mesenchymal MSC in collagen gels were found to show higher contraction rates than described for fibroblasts [41]. Collagen gel contraction is commonly used as a measure of cell-mediated matrix reorganization [42], therefore our theorem of a differentiation process in the TLC is further supported.

Among the specific markers described to be expressed by tendon tissue are scleraxis (Scx), tenomodulin (TNMD), thrombospondin-4 (TSP-4), tenascin-C (TNC), type I collagen (Col I) and type III collagen (Col III). However, they show different expression level and pattern dependent from kind of tissue or duration of cultivation ex vivo [43]. Specific markers for a differentiation towards tenocytes were found in TLCs differentiated from ASCs.

Col I is of utmost importance for the stability of tendons as well as remodeling of the ECM during tendon healing as it makes up more than 90% of the structural elements in normal tendon tissue [44]. Expression of Col I and III is up-regulated as a response to mechanical loading, which is consistent with our study as we found qualitatively more Col I- and Col III-positive cells in TLC with mechanical stimulation [45,46]. This is probably due to adaption by strengthening of the ECM.

Regarding the course of markers, it has to be considered that ASCs as a stem cell population were deployed to differentiate into tendon tissue instead of mature tenocytes or tendon progenitor cells. It has been reported that there are certain differences whether tendon tissue samples or tenocytes in cell cultures were investigated. When tenocytes were

isolated and cultivated, only the markers Col I, Col III and TNC were significantly higher than in MSC cultures while Scx, TNMD, TSP-4 dropped immediately after plating isolated tenocytes into Passage 1 [43]. As we investigated TLC derived from differentiated ASC and not in vivo tissue samples, it was not surprising that these markers were positive at all.

While they have been used to engineer tendon tissue, either co-cultures or addition of growth factors (i.e., bone morphogenetic ptotein-12) were applied to achieve TLCs [47,48]. ASCs have been described to support tendon healing in vivo by inducing neovascularization [49]. To our knowledge, this is the first study using ASC for TLC engineering without supplementary addition of growth factors. However, one limitation is the use of ASC that came from only one fat tissue donor. As described elsewhere, the age of the donor, the localization of adipose tissue harvesting for stem cell isolation, and other factors play a crucial role for the multipotency of ASC [25,50]. The presented study was approved by the ethics committee of Hannover Medical School therefore no changes could be made to the experimental setup. For future experiments, cell pooling would be useful to eliminate donor-specific differences.

Spider silk is known as the world's toughest biomaterial surpassing the tensile strength of many biomaterials and the breaking strength of any artificial material reaching up to 520 MJ/kg^3 [51]. In earlier studies utilizing spider silk as tendon suture material, no significant decrease in failure load was reported after 1000 fatigue cycles of strain [36]. Therefore, it seems predestined for the use of tendon tissue engineering. A electro spun composite of spider silk and carbon nano-tubes was employed in a robotic human hand and withstood up to 40,000 bending-stretching cycles while at the same time being able to transmit force as well as electronic signals in term of a feedback system [52]. This application implies possible modifications of native spider silk as well as use of those composites for use in myoelectric prosthetics. On the other hand, further investigations optimizing the conditions of tissue engineering of the pilot study presented herein might lead to optimization of TLC for early in vitro-to-in vivo-strategies. Future studies could also focus on the use of spider silk proteins for 3D tissue printing for example using silk inks [53,54]. How, beyond the hype and before 3D bioprinted organs are ready to be transplanted into humans, several important ethical issues and regulatory concerns need to be addressed [55,56].

Another limitation of the study remains the unclear immunocompatibility of the developed TLC. Since the present study is a proof-of-concept study, further investigations are necessary to make conclusive statements about the biocompatibility of the TLC. The use of rat collagen type I would most likely lead to an immunological reaction of the recipient organism, so that an intervention in the intrinsic alloreactivity, e.g., by the use of immunosuppressive drugs, would be necessary. It is also conceivable that rat collagen type I is not an optimal matrix material [57]. As published elsewhere, collagens of jellyfish have been intensively studied and showed nearly complete degradation post implantation after 60 days in a rodent model. Furthermore, the degradation process ended in a vessel-rich connective tissue that is understood to be an optimal basis for tissue regeneration [58]. Due to its proven promising immunological properties of native spider silk of species *Nephila edulis*, it is possible to speak overall of a future-oriented biomaterial [22]. However, further analyses are required to determine the optimal composition of the TLC presented here.

In the present study, Scx could not be detected in the constructs and no quantitative values could be determined due to interferences of spider silk fibers in polymerase chain reaction (PCR) analysis. Therefore, no definitive conclusion can be made of the influence of mechanical stimulation regarding whether it is superior in terms of expression of different tendon specific markers. However, morphologic analysis revealed better cell alignment towards a tenocyte phenotype.

Author Contributions: Conceptualization, J.W.K. and F.S.; methodology, F.S., J.W.K.; software, F.S., S.S., B.W.; validation S.S., B.W., and P.M.V.; formal analysis, F.S., J.W.K., S.S.; investigation, F.S., B.W., C.P., J.W.K.; resources, S.S., P.M.V.; data curation, F.S.; writing—original draft preparation, F.S. and J.W.K.; writing—review and editing, C.P., B.W., P.M.V., and S.S.; visualization, F.S.; supervision, J.W.K.; project administration, J.W.K.; funding acquisition, J.W.K. All authors have read and agreed to the published version of the manuscript.

Funding: Parts of this study were funded by achievement-orientated internal funding of Hannover Medical School (HILF) from a grant (No. 79470013) achieved by J.W.K. We acknowledge support by the German Research Foundation (DFG) and the Open Access Publication Fund of Hannover Medical School (MHH).

Institutional Review Board Statement: The study was conducted according to the guidelines of the Declaration of Helsinki, and approved by the Ethics Committee of Hannover Medical School (Ethics Approval No. 3475-2017; Date of approval: 15 February 2017).

Informed Consent Statement: Informed consent was obtained of all subjects involved in the study.

Data Availability Statement: The data presented in this study are available on request from the corresponding author. The data are not publicly available due to privacy reasons.

Acknowledgments: In memory of Kerstin Reimers-Fadhlaoui (†23.12.2015), former Head of the Experimental Department of Plastic, Aesthetic, Hand and Reconstructive Surgery at Hannover Medical School. The authors are grateful to Andrea Lazaridis for her excellent technical support. Additionally, the authors want to thank the Central Research Devices Service Unit of Hannover Medical School for the building of the custom-designed bioreactor.

Conflicts of Interest: The authors declare no conflict of interest. The funders had no role in the design of the study; in the collection, analyses, or interpretation of data; in the writing of the manuscript, or in the decision to publish the results.

References

1. Cowin, S.C. Tissue Growth and Remodeling. *Annu. Rev. Biomed. Eng.* **2004**, *6*, 77–107. [CrossRef]
2. Nichols, A.E.C.; Best, K.T.; Loiselle, A.E. The cellular basis of fibrotic tendon healing: Challenges and opportunities. *Transl. Res.* **2019**, *209*, 156–168. [CrossRef]
3. Fernandes, T.L.; De Santanna, J.P.C.; Frisene, I.; Gazarini, J.P.; Pinheiro, C.C.G.; Gomoll, A.H.; Lattermann, C.; Hernandez, A.J.; Bueno, D.F. Systematic Review of Human Dental Pulp Stem Cells for Cartilage Regeneration. *Tissue Eng. Part B Rev.* **2020**, *26*, 1–12. [CrossRef]
4. Sharma, P.; Maffulli, N. Biology of tendon injury: Healing, modeling and remodeling. *J. Musculoskelet. Neuronal Interact.* **2006**, *6*, 181–190.
5. Murakami, A.M.; Kompel, A.J.; Engebretsen, L.; Li, X.; Forster, B.B.; Crema, M.D.; Hayashi, D.; Jarraya, M.; Roemer, F.W.; Guermazi, A. The epidemiology of MRI detected shoulder injuries in athletes participating in the Rio de Janeiro 2016 Summer Olympics. *BMC Musculoskelet. Disord.* **2018**, *19*, 296. [CrossRef]
6. Li, L.T.; Bokshan, S.L.; Ready, L.V.; Owens, B.D. The primary cost drivers of arthroscopic rotator cuff repair surgery: A cost-minimization analysis of 40,618 cases. *J. Shoulder Elb. Surg.* **2019**, *28*, 1977–1982. [CrossRef]
7. Lim, W.L.; Liau, L.L.; Ng, M.H.; Chowdhury, S.R.; Law, J.X. Current Progress in Tendon and Ligament Tissue Engineering. *Tissue Eng. Regen. Med.* **2019**, *16*, 549–571. [CrossRef] [PubMed]
8. Vasiliadis, A.V.; Katakalos, K.V. The Role of Scaffolds in Tendon Tissue Engineering. *J. Funct. Biomater.* **2020**, *11*, 78. [CrossRef] [PubMed]
9. Doroski, D.M.; Levenston, M.E.; Temenoff, J.S. Cyclic Tensile Culture Promotes Fibroblastic Differentiation of Marrow Stromal Cells Encapsulated in Poly(Ethylene Glycol)-Based Hydrogels. *Tissue Eng. Part A* **2010**, *16*, 3457–3466. [CrossRef] [PubMed]
10. Messenger, M.P.; Raïf, E.M.; Seedhom, B.B.; Brookes, S.J. Enamel matrix derivative enhances tissue formation around scaffolds used for tissue engineering of ligaments. *J. Tissue Eng. Regen. Med.* **2010**, *4*, 96–104. [CrossRef] [PubMed]
11. Mizuno, S.; Tateishi, T.; Ushida, T.; Glowacki, J. Hydrostatic fluid pressure enhances matrix synthesis and accumulation by bovine chondrocytes in three-dimensional culture. *J. Cell. Physiol.* **2002**, *193*, 319–327. [CrossRef] [PubMed]
12. Ogawa, R.; Mizuno, S.; Murphy, G.F.; Orgill, D. The Effect of Hydrostatic Pressure on Three-Dimensional Chondroinduction of Human Adipose-Derived Stem Cells. *Tissue Eng. Part A* **2009**, *15*, 2937–2945. [CrossRef] [PubMed]
13. Chandran, P.L.; Barocas, V.H. Microstructural Mechanics of Collagen Gels in Confined Compression: Poroelasticity, Viscoelasticity, and Collapse. *J. Biomech. Eng.* **2004**, *126*, 152–166. [CrossRef] [PubMed]
14. Sellaro, T.L.; Hildebrand, D.; Lu, Q.; Vyavahare, N.; Scott, M.; Sacks, M.S. Effects of collagen fiber orientation on the response of biologically derived soft tissue biomaterials to cyclic loading. *J. Biomed. Mater. Res. Part A* **2007**, *80*, 194–205. [CrossRef] [PubMed]

15. Arnoczky, S.P.; Lavagnino, M.; Whallon, J.H.; Hoonjan, A. In situ cell nucleus deformation in tendons under tensile load; a morphological analysis using confocal laser microscopy. *J. Orthop. Res.* **2002**, *20*, 29–35. [CrossRef]
16. Dyment, N.; Barrett, J.G.; Awad, H.A.; Bautista, C.A.; Banes, A.J.; Butler, D.L. A brief history of tendon and ligament bioreactors: Impact and future prospects. *J. Orthop. Res.* **2020**, *38*, 2318–2330. [CrossRef]
17. Santos, M.L.; Rodrigues, M.T.; Domingues, R.M.A.; Reis, R.L.; Gomes, M.E. Biomaterials as Tendon and Ligament Substitutes: Current Developments. In *Regenerative Strategies for the Treatment of Knee Joint Disabilities*; Oliveira, J., Reis, R., Eds.; Springer: Cham, Switzerland, 2017; Volume 21; pp. 349–371.
18. Kuo, C.K.; Marturano, J.E.; Tuan, R.S. Novel strategies in tendon and ligament tissue engineering: Advanced biomaterials and regeneration motifs. *BMC Sports Sci. Med. Rehabil.* **2010**, *2*, 20. [CrossRef]
19. Gosline, J.; Guerette, P.A.; Ortlepp, C.S.; Savage, K.N. The mechanical design of spider silks: From fibroin sequence to mechanical function. *J. Exp. Biol.* **1999**, *202*, 3295–3303.
20. Lewis, R.V. Spider Silk: Ancient Ideas for New Biomaterials. *Chem. Rev.* **2006**, *106*, 3762–3774. [CrossRef]
21. Schäfer-Nolte, F.; Hennecke, K.; Reimers, K.; Schnabel, R.; Allmeling, C.; Vogt, P.; Kuhbier, J.; Mirastschijski, U. Biomechanics and Biocompatibility of Woven Spider Silk Meshes During Remodeling in a Rodent Fascia Replacement Model. *Ann. Surg.* **2014**, *259*, 781–792. [CrossRef]
22. Kuhbier, J.; Coger, V.; Mueller, J.; Liebsch, C.; Schlottmann, F.; Bucan, V.; Vogt, P.M.; Strauss, S. Influence of direct or indirect contact for the cytotoxicity and blood compatibility of spider silk. *J. Mater. Sci. Mater. Electron.* **2017**, *28*, 127. [CrossRef] [PubMed]
23. Afizah, H.; Yang, Z.; Hui, J.H.; Ouyang, H.-W.; Lee, E.H. A Comparison Between the Chondrogenic Potential of Human Bone Marrow Stem Cells (BMSCs) and Adipose-Derived Stem Cells (ADSCs) Taken from the Same Donors. *Tissue Eng.* **2007**, *13*, 659–666. [CrossRef] [PubMed]
24. Vuornos, K.; Björninen, M.; Talvitie, E.; Paakinaho, K.; Kellomäki, M.; Huhtala, H.; Miettinen, S.; Seppänen-Kaijansinkko, R.; Haimi, S. Human Adipose Stem Cells Differentiated on Braided Polylactide Scaffolds Is a Potential Approach for Tendon Tissue Engineering. *Tissue Eng. Part A* **2016**, *22*, 513–523. [CrossRef] [PubMed]
25. Kuhbier, J.W.; Weyand, B.; Radtke, C.; Vogt, P.M.; Kasper, C.; Reimers, K. Isolation, Characterization, Differentiation, and Application of Adipose-Derived Stem Cells. *Bioreact. Syst. Tissue Eng. II* **2010**, *123*, 55–105. [CrossRef]
26. Rajan, N.; Habermehl, J.; Coté, M.-F.; Doillon, C.J.; Mantovani, D. Preparation of ready-to-use, storable and reconstituted type I collagen from rat tail tendon for tissue engineering applications. *Nat. Protoc.* **2006**, *1*, 2753–2758. [CrossRef]
27. Desjardins, P.; Hansen, J.B.; Allen, M. Microvolume Protein Concentration Determination Using the NanoDrop 2000c Spectrophotometer. *J. Vis. Exp.* **2009**, e1610. [CrossRef]
28. Liebsch, C.; Fliess, M.; Kuhbier, J.W.; Vogt, P.M.; Strauß, S. Nephila edulis—Breeding and care under laboratory conditions. *Dev. Genes Evol.* **2020**, *230*, 203–211. [CrossRef]
29. Kuhbier, J.W.; Allmeling, C.; Reimers, K.; Hillmer, A.; Kasper, C.; Menger, B.; Brandes, G.; Guggenheim, M.; Vogt, P.M. Interactions between Spider Silk and Cells—NIH/3T3 Fibroblasts Seeded on Miniature Weaving Frames. *PLoS ONE* **2010**, *5*, e12032. [CrossRef]
30. Kall, S.; Noth, U.; Reimers, K.; Choi, C.Y.U.; Muehlberger, T.; Allmeling, C.; Jahn, S.; Heymer, A.; Vogt, P.M. In vitroHerstellung von Sehnenkonstrukten aus humanen mesenchymalen Stammzellen und einem Kollagen Typ I Gel. *Handchir. Mikrochir. Plast. Chir.* **2004**, *36*, 205–211. [CrossRef]
31. Ratzlaff, M.H.; Grant, B.D.; Rathgeber-Lawrence, R.; Kunka, K.L. Stride rates of horses trotting and cantering on a treadmill. *J. Equine Vet. Sci.* **1995**, *15*, 279–283. [CrossRef]
32. Chen, X.; Yin, Z.; Chen, J.-L.; Shen, W.-L.; Liu, H.-H.; Tang, Q.-M.; Fang, Z.; Lu, L.-R.; Ji, J.; Ouyang, H.-W. Force and scleraxis synergistically promote the commitment of human ES cells derived MSCs to tenocytes. *Sci. Rep.* **2012**, *2*, 977. [CrossRef] [PubMed]
33. Atkinson, F.; Evans, R.; Guest, J.E.; Bavin, E.P.; Cacador, D.; Holland, C.; Guest, D.J. Cyclical strain improves artificial equine tendon constructs in vitro. *J. Tissue Eng. Regen. Med.* **2020**, *14*, 690–700. [CrossRef] [PubMed]
34. Legerlotz, K.; Jones, G.C.; Screen, H.R.C.; Riley, G.P. Cyclic loading of tendon fascicles using a novel fatigue loading system increases interleukin-6 expression by tenocytes. *Scand. J. Med. Sci. Sports* **2013**, *23*, 31–37. [CrossRef] [PubMed]
35. Chaudhury, S.; Holland, C.; Thompson, M.; Vollrath, F.; Carr, A.J. Tensile and shear mechanical properties of rotator cuff repair patches. *J. Shoulder Elb. Surg.* **2012**, *21*, 1168–1176. [CrossRef] [PubMed]
36. Hennecke, K.; Redeker, J.; Kuhbier, J.W.; Strauss, S.; Allmeling, C.; Kasper, C.; Reimers, K.; Vogt, P.M. Bundles of Spider Silk, Braided into Sutures, Resist Basic Cyclic Tests: Potential Use for Flexor Tendon Repair. *PLoS ONE* **2013**, *8*, e61100. [CrossRef] [PubMed]
37. Tohidnezhad, M.; Zander, J.; Slowik, A.; Kubo, Y.; Dursun, G.; Willenberg, W.; Zendedel, A.; Kweider, N.; Stoffel, M.; Pufe, T. Impact of Uniaxial Stretching on Both Gliding and Traction Areas of Tendon Explants in a Novel Bioreactor. *Int. J. Mol. Sci.* **2020**, *21*, 2925. [CrossRef]
38. Michal, C.A.; Simmons, A.; Chew, B.; Zax, D.; Jelinski, L. Presence of phosphorus in Nephila clavipes dragline silk. *Biophys. J.* **1996**, *70*, 489–493. [CrossRef]
39. Shen, Y.; Zhu, D.; Lu, W.; Liu, B.; Li, Y.; Cao, S. The Characteristics of Intrinsic Fluorescence of Type I Collagen Influenced by Collagenase I. *Appl. Sci.* **2018**, *8*, 1947. [CrossRef]
40. Awad, H.A.; Butler, D.L.; Harris, M.T.; Ibrahim, R.E.; Wu, Y.; Young, R.G.; Kadiyala, S.; Boivin, G.P. In vitro characterization of mesenchymal stem cell-seeded collagen scaffolds for tendon repair: Effects of initial seeding density on contraction kinetics. *J. Biomed. Mater. Res.* **2000**, *51*, 233–240. [CrossRef]

41. Hilton, S.A.; Dewberry, L.C.; Hodges, M.M.; Hu, J.; Xu, J.; Liechty, K.W.; Zgheib, C. Mesenchymal stromal cells contract collagen more efficiently than dermal fibroblasts: Implications for cytotherapy. *PLoS ONE* **2019**, *14*, e0218536. [CrossRef]
42. Yang, T.-H.; Thoreson, A.R.; Gingery, A.; Larson, D.R.; Passe, S.M.; An, K.-N.; Zhao, C.; Amadio, P.C. Collagen gel contraction as a measure of fibroblast function in an animal model of subsynovial connective tissue fibrosis. *J. Orthop. Res.* **2015**, *33*, 668–674. [CrossRef] [PubMed]
43. Jo, C.H.; Lim, H.-J.; Yoon, K.S. Characterization of Tendon-Specific Markers in Various Human Tissues, Tenocytes and Mesenchymal Stem Cells. *Tissue Eng. Regen. Med.* **2019**, *16*, 151–159. [CrossRef] [PubMed]
44. Doral, M.N.; Alam, M.; Bozkurt, M.; Turhan, E.; Atay, O.A.; Dönmez, G.; Maffulli, N. Functional anatomy of the Achilles tendon. *Knee Surg. Sports Traumatol. Arthrosc.* **2010**, *18*, 638–643. [CrossRef] [PubMed]
45. Zhang, J.; Wang, J.H.-C. The Effects of Mechanical Loading on Tendons—An In Vivo and In Vitro Model Study. *PLoS ONE* **2013**, *8*, e71740. [CrossRef] [PubMed]
46. Fleischhacker, V.; Klatte-Schulz, F.; Minkwitz, S.; Schmock, A.; Rummler, M.; Seliger, A.; Willie, B.M.; Wildemann, B. In Vivo and In Vitro Mechanical Loading of Mouse Achilles Tendons and Tenocytes—A Pilot Study. *Int. J. Mol. Sci.* **2020**, *21*, 1313. [CrossRef]
47. Long, C.; Wang, Z.; Legrand, A.; Chattopadhyay, A.; Chang, J.; Fox, P. Tendon Tissue Engineering: Mechanism and Effects of Human Tenocyte Coculture With Adipose-Derived Stem Cells. *J. Hand Surg.* **2018**, *43*, 183.e1–183.e9. [CrossRef]
48. Shen, H.; Gelberman, R.H.; Silva, M.J.; Sakiyama-Elbert, S.E.; Thomopoulos, S. BMP12 induces tenogenic differentiation of adipose-derived stromal cells. *PLoS ONE* **2013**, *8*, e77613. [CrossRef]
49. Kokubu, S.; Inaki, R.; Hoshi, K.; Hikita, A. Adipose-derived stem cells improve tendon repair and prevent ectopic ossification in tendinopathy by inhibiting inflammation and inducing neovascularization in the early stage of tendon healing. *Regen. Ther.* **2020**, *14*, 103–110. [CrossRef]
50. Kuhbier, J.W.; Weyand, B.; Sorg, H.; Radtke, C.; Vogt, P.M.; Reimers, K. Stem cells from fatty tissue: A new resource for regenerative medicine? *Chir. Z. Alle Geb. Oper. Medizen* **2010**, *81*, 826–832. [CrossRef]
51. Agnarsson, I.; Kuntner, M.; Blackledge, T.A. Bioprospecting Finds the Toughest Biological Material: Extraordinary Silk from a Giant Riverine Orb Spider. *PLoS ONE* **2010**, *5*, e11234. [CrossRef]
52. Pan, L.; Wang, F.; Cheng, Y.; Leow, W.R.; Zhang, Y.-W.; Wang, M.; Cai, P.; Ji, B.; Li, D.; Chen, X. A supertough electro-tendon based on spider silk composites. *Nat. Commun.* **2020**, *11*, 1332. [CrossRef] [PubMed]
53. Moore, C.A.; Shah, N.N.; Smith, C.P.; Rameshwar, P. 3D Bioprinting and Stem Cells. In *Methods in Molecular Biology*; Clifton, N.J., Ed.; Humana Press: New York, NY, USA, 2018; Volume 1842; pp. 93–103.
54. Agostinacchio, F.; Mu, X.; Dirè, S.; Motta, A.; Kaplan, D.L. In Situ 3D Printing: Opportunities with Silk Inks. *Trends Biotechnol.* **2020**. [CrossRef] [PubMed]
55. Ng, W.L.; Chua, C.K.; Shen, Y.-F. Print Me An Organ! Why We Are Not There Yet. *Prog. Polym. Sci.* **2019**, *97*, 101145. [CrossRef]
56. Gilbert, F.; O'Connell, C.D.; Mladenovska, T.; Dodds, S. Print Me an Organ? Ethical and Regulatory Issues Emerging from 3D Bioprinting in Medicine. *Sci. Eng. Ethic* **2018**, *24*, 73–91. [CrossRef] [PubMed]
57. Sapudom, J.; Mohamed, W.K.E.; Garcia-Sabaté, A.; Alatoom, A.; Karaman, S.; Mahtani, N.; Teo, J.C.M. Collagen Fibril Density Modulates Macrophage Activation and Cellular Functions during Tissue Repair. *Bioengineering* **2020**, *7*, 33. [CrossRef]
58. Flaig, I.; Radenković, M.; Najman, S.; Proehl, A.; Jung, O.; Barbeck, M. In Vivo Analysis of the Biocompatibility and Immune Response of Jellyfish Collagen Scaffolds and its Suitability for Bone Regeneration. *Int. J. Mol. Sci.* **2020**, *21*, 4518. [CrossRef]